The Transitional Junction: A New Functional Subcellular Domain at the Intercalated Disc

**Pauline M. Bennett,* Alison M. Maggs,* Anthony J. Baines,†
and Jennifer C. Pinder***

*Randall Division of Cell and Molecular Biophysics, GKT School of Biomedical Sciences, King's College London, Guy's Campus, London SE1 1UL, United Kingdom; and †Department of Biosciences, University of Kent, Canterbury CT2 7NJ, United Kingdom

We define here a previously unrecognized structural element close to the heart muscle plasma membrane at the intercalated disc where the myofibrils lead into the adherens junction. At this location, the plasma membrane is extensively folded. Immunofluorescence and immunogold electron microscopy reveal a spectrin-rich domain at the apex of the folds. These domains occur at the axial level of what would be the final Z-disc of the terminal sarcomere in the myofibril, although there is no Z-disc–like structure there. However, a sharp transitional boundary lies between the myofibrillar I-band and intercalated disc thin filaments, identifiable by the presence of Z-disc proteins, α-actinin, and N-terminal titin. This allows for the usual elastic positioning of the A-band in the final sarcomere, whereas the transduction of the contractile force normally associated with the Z-disc is transferred to the adherens junctions at the plasma membrane. The axial conjunction of the transitional junction with the spectrin-rich domains suggests a mechanism for direct communication between intercalated disc and contractile apparatus. In particular, it provides a means for sarcomeres to be added to the ends of the cells during growth. This is of particular relevance to understanding myocyte elongation in dilated cardiomyopathy.

INTRODUCTION

Mechanical coupling and chemical communication between cardiac muscle cells are encompassed by a structure called the intercalated disc (ID). It is known that mutations or deficiencies in its constituent proteins give rise to cardiomyopathy or other fatal defects. The ID is a highly involuted element located at the distal ends of the bipolar muscle cells. During cardiac contractions, the ID must have an adhesive function while also transmitting and coordinating essential signaling events. To fulfill these roles the ID is highly organized structurally. Thus, complex ID domains alternate to afford both mechanical strength and electrical and chemical communication across the membranes of adjacent cells. There are a number of reports of heart disease associated with structural change in the ID (for a review, see Perriard *et al.*, 2003). For example, in mice with inactivated expression of the intercalated disc protein N-cadherin, the embryo dies (Radice *et al.*, 1997). In contrast, knockout of expression of the β-spectrin binding protein muscle LIM protein (MLP) leads to overexpression of some of the ID proteins, especially those of the adherens junction, and results in dilated cardiomyopathy (DCM) (Arber *et al.*, 1997; Ehler *et al.*, 2001).

Address correspondence to: Pauline Bennett (pauline.bennett@kcl.ac.uk).

Abbreviations used: DCM, dilated cardiomyopathy; ID, intercalated disc.

This holds also for the tropomodulin overexpressing transgenic mouse (Sussman *et al.*, 1998; Ehler *et al.*, 2001).

In the light microscope in longitudinal sections, the ID is seen as a transverse dense line of mass with occasional steps at irregular intervals (for review, see Forbes and Sperelakis, 1985). At higher magnification in the electron microscope, the membrane on the transverse treads describes complex folds, whereas the risers are straight (Figure 1). In three dimensions, the treads may be likened to an egg box with troughs and peaks where the cells interdigitate. Within this complicated arrangement three specialized membrane-associated regions have been described: adherens junctions, desmosomes, and gap junctions. In addition, there are apparently unspecialized regions of no known function. As seen in Figure 1B, at the gap junction (g) which mostly occurs in the riser regions, the plasma membranes of the two adjacent cells come close together with an increased density. The desmosome (d) is usually seen as a dense but well-ordered structure with extra mass in the interstitial gap between the membranes. The membrane here is usually straight and most frequently occurs in nonfibrillar parts of the ID, e.g., where there are stacks of mitochondria. Finally, the adherens junctions (a) are found at the end of myofibrils and are characterized by considerable extra, somewhat fuzzy, mass close to the plasma membrane (known as the cytoplasmic plaque). The ID at this point has been termed the interfibrillar region (Forbes and Sperelakis, 1985), and it is this region with which we are concerned here.

In support of the structural complexity, a wide array of proteins have been associated with the ID by immunofluorescence and other means, many of which are located in the specialized membrane junctions. The locations and functions of other proteins are uncertain. One such protein is the mem-

brane-bound protein, spectrin (Messina and Lemanski, 1989; Isayama *et al.*, 1993; Bennett *et al.*, 2004; Baines and Pinder, 2005), a heterodimeric (αβ) elongated actin-binding protein (for review, see Bennett and Baines, 2001). The dimers associate head-to-head to form tetramers that bind to filamentous actin at their distal ends. The resulting network is the basis of the elasticity and shear-resistance of the erythrocyte membrane. In the erythrocyte, this meshwork, together with a number of other proteins, forms a dynamic membrane-associated cytoskeleton that helps the cell withstand the forces experienced in its passage through capillaries. How this relates to the role of spectrin in the intercalated disc is not clear, but it implies the presence of a type of domain other than the previously described junctions. Whatever its role, spectrin's importance in cardiac tissue has been clearly demonstrated; in mouse a null mutation in the βII-spectrin gene produces nonviable animals that die in midgestation from defects that include heart malformation (Tang *et al.*, 2003).

Spectrin has two α-chain and five β-chain isoforms in vertebrates (for review, see Bennett and Baines, 2001), four of which, αI and βI (the erythrocyte isoforms) and αII and βII (also known as α- and β-fodrin), have been identified in heart. They distribute differentially in cardiac muscle, although the precise location of each is not clear (for review, see Baines and Pinder, 2005). All but βII-spectrin are found on the lateral plasma membrane, but both βII-spectrin splice variants occur in the cardiomyocyte at the ID, within the cell at the Z-disc level, and weakly elsewhere (Hayes *et al.*, 2000; Baines and Pinder, 2005). Furthermore, we recently also found the αII isoform at the ID and within the cell at the edges of the myofibrils, mainly at the Z-disc level (Bennett *et al.*, 2004). The immunofluorescence staining of αII-spectrin at the ID is much stronger than that at the Z-disc level. Immunogold labeling showed it to be associated with the transverse pleated treads of the ID (Bennett *et al.*, 2004).

The association of spectrin with the Z-disc of the myofibrils within cardiomyocytes suggests that there may be a similar association at or near the ID. However, little is known about the junction between the myofibrillar structure and the ID. It is striking that the fibrils maintain their ordered sarcomeric arrangement in a region adjacent to the apparently unordered ID (Figure 1). This is in the absence of a terminal Z-disc. It is clear that the thin actin filaments leave the terminal half-sarcomere and pass into the ID, where they insert into the adherens junctions at the membrane (Forbes and Sperelakis, 1985; Yamaguchi *et al.*, 1988). The longitudinal tension generated by the myofibrils is evidently transmitted across the cell membranes at these junctions. It is in this interfibrillary region that the ID membrane is most convoluted. Furthermore, the apices of the folds are approximately at the axial level that the Z-disc would have occupied, had it been present, implying a likely interaction between the myofibril and an ID membrane domain.

We have investigated the distribution and position of spectrin within the ID as well as its relationship to the known membrane junctional complexes, in particular the adherens junction, using immunofluorescence and immunogold electron microscopy. We find that although the components of the adherens junctions, such as vinculin, can be considered to be distributed uniformly over much of the ID membrane, spectrin is confined to the axial extremes of the ID where it lies on the outer convex folds of the membrane. To determine the relationship of cardiac ID spectrin to the myofibrillar structure, we have labeled sarcomeric and Z-disc proteins and find we can accurately define the junction between the myofibrillar thin filaments and the ID filaments. From this, we define the presence of a new subcellular structure that we have named the "transitional junction," whose axial position is closely correlated with that of spectrin. The transitional junction also acts as an anchor point for titin and hence for maintaining the ordered array of the terminal A-band.

MATERIALS AND METHODS

Normal Sections

Hearts from BalbC or C57B mice were perfused briefly in phosphate-buffered saline containing 1 mM sodium azide and 1 mM EGTA and then with 2% paraformaldehyde in 0.1 M phosphate buffer, pH 7.4, before excision. Small pieces (~1 mm³) of left ventricle were subsequently fixed in 2.5% glutaraldehyde in the same buffer for 2 h on ice. Specimens were washed, postfixed in osmium, dehydrated in alcohol, and embedded in Araldite. Thin sections were stained with potassium permanganate followed by lead citrate.

Cryosections

Thin cryosections were obtained as described in Bennett *et al.* (2004). Hearts from adult mice were perfused as described above and fixed by 2% paraformaldehyde in 0.1 M sodium phosphate buffer, pH 7.4. Hearts were excised and the left ventricle was dissected out and cut into small pieces that were further fixed for 30 min on ice. The pieces were infiltrated overnight with 2.3 M sucrose before mounting on pins and freezing in liquid nitrogen.

For microscopy, sections were obtained on a Leica ultramicrotome with a cryo attachment. They were picked up on drops of 1% methylcellulose/1.15 M sucrose. Semithin sections, 200 nm in thickness, were transferred to gelatin-coated slides for immunofluorescence, and thin sections, 70 nm in thickness, were transferred to Formvar/carbon-coated grids for electron microscopy. They were stored at 4°C.

Antibodies

The following antibodies were used. T12, a mouse monoclonal antibody specific for the I-band domain of titin close to the Z-line was a kind gift from Dr. M. Gautel (King's College London, London, United Kingdom) (Furst *et al.*, 1988). I20/I22, a rabbit polyclonal antibody specific for an I-band region of titin close to the end of the thick filament (Linke *et al.*, 1998), was kindly supplied by Dr. W. Linke (University of Muenster, Muenster, Germany). Anti-αII-spectrin was a rabbit polyclonal antibody raised against the Src homology 3 domain (Nicolas *et al.*, 1998) and was kindly supplied by Dr. M.-C. Lecomte (Inserm U665, Paris, France). Mouse monoclonal anti-vinculin (V4505), anti-tropomyosin (TM311), and anti-α-actinin (EA-53) as well as rabbit polyclonal anti-β-catenin (C2206) were obtained from Sigma-Aldrich (St. Louis, MO). Mouse monoclonal anti-αI-spectrin (17C7) came from Abcam (Cambridge, United Kingdom). Mouse monoclonal antibodies against ZASP (Faulkner *et al.*, 1999) and cardiac troponin I (Saggin *et al.*, 1989) were generous gifts from Drs. G. Faulkner (International Centre for Genetic Engineering and Biotechnology, Trieste, Italy) and E. Ehler (King's College London, London, United Kingdom).

For light microscopy, the secondary antibodies were obtained from Molecular Probes and were either goat anti-mouse IgG conjugated to Alexa Fluor 568, or Alexa Fluor 488 or goat anti-rabbit IgG conjugated to Alexa Fluor 488 or Marina Blue. Some sections were also labeled with phalloidin complexed to rhodamine. Sections were mounted with Vectashield (Vector Laboratories, Burlingame, CA), usually containing 4,6-diamidino-2-phenylindole. Specimens were viewed in a Zeiss Axiovert 200M epifluoresence microscope fitted with a Plan Apochromat 63×/1.32 oil immersion objective. Images were recorded using an AxioCam HRm digital camera fitted to the microscope and controlled with the Zeiss AxioVision LE 4.2 software package.

For immunogold labeling, protein A tagged with 10-nm gold particles (PAG10) was used with rabbit antibodies (Department of Cell Biology, Utrecht University, Utrecht, The Netherlands). For mouse and double labeling experiments, goat anti-mouse coupled to 5-nm gold (GAR5) or goat anti-rabbit coupled to 10-nm gold (GAR10) was used (Biocell, Cardiff, UK). Specimens were viewed either in a JEOL 200CX or a Hitachi 7600 transmission electron microscope (Centre for Ultrastructural Imaging, King's College London, London, United Kingdom).

Analysis

Immunofluorescence. For measurements, digital images were displayed in Photoshop (Adobe Systems, Mountain View, CA), rotated to align the fibril axis with the horizontal, and the x positions of the stripes were determined in pixels. The separation of the antibody-labeled stripes to either side of the ID was measured in an area showing Z-discs from abutting cells as well. This enabled the position of several Z-discs in each cell to either side of the ID to be measured and used to obtain a least-squares fit to a straight line and to calculate the expected positions of the ID doublet stripes were they to be at the
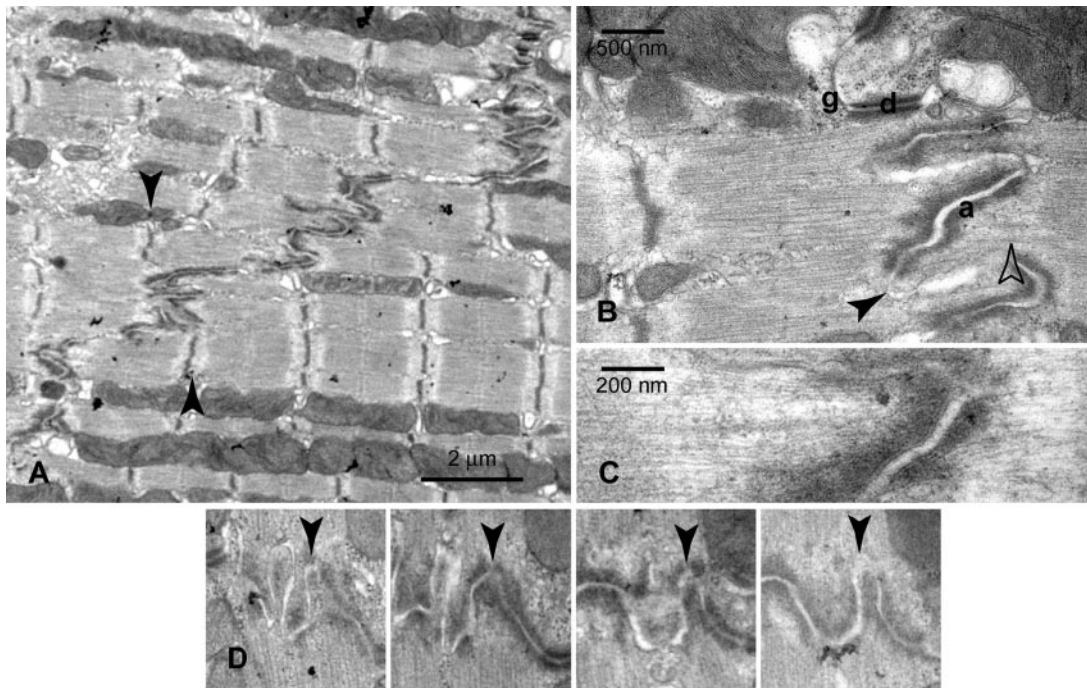
Figure 1. (A) Electron micrograph of part of an intercalated disc between two cardiac cells showing the stairlike steps across the cells. Arrows indicate how the axial extremes of one of the transverse regions correspond to the position of the Z-discs of neighboring myofibrils. (B) Higher magnification of one transverse region showing adherens junctions (a), desmosomes (d), gap junction (g), and general apparently unspecialized plasma membrane at the tip of the folds (arrowhead). Also notable is the absence of Z-discs when myofibrils feed into the ID (open arrowhead). (C) Higher magnification view illustrating the continuity of thin filaments from sarcomere to ID membrane. (D) A series of four sections ~100 nm apart showing the development of one of the folds (arrowhead) and the absence of plaque at the top of the fold in the final image.

position of the Z-discs. The calculated separation of the two was plotted against the measured difference in spacing (Figure 4).

Electron Microscopy. Measurements were made on digitized electron micrographs with a pixel size of 1 to 2 nm displayed using Scion Image software (Scion, Frederick, MD). The distance of gold particles from the ID membrane was taken from the center of the gap between the abutting plasma membranes to the gold particle in a direction perpendicular to the plasma membrane.

The axial distribution of gold particles across the ID was measured on micrographs that showed enough sarcomeric structure such that at least a half-sarcomere length (from Z-disc to M-lines) on each side of the ID could be measured. The edges of the ID were taken to be a whole sarcomere length from the nearest Z-discs. In this way the width and position of the ID was determined and the position of the gold particles was measured axially from the center of the ID.

Modeling the Axial Distribution of ID Membrane Proteins. It is instructive to consider what the distribution of label would be expected to be for an antigen on the convoluted plasma membrane of the ID. We have likened the form of the membrane to that of an egg box. It is of course much less ordered but for argument's sake, we have assumed a regular arrangement of ups and downs. We can approximate this arrangement with a series of smooth-topped cones so that a plane through the peaks shows a sinusoidal curve (Figure 2A). Using this curve, we can calculate the area of membrane available at each axial level, y, as $\Delta A(y) = 2\pi x \, \Delta L$. Using the equations $(\Delta L)^2 = (\Delta x)^2 + (\Delta y)^2$ and $y = \cos x$, we can show that $\Delta A(y) = [(2 - y^2)/(1 - y^2)]^{1/2} 2\pi \cos^{-1} y$.

A plot of ΔA against y is shown in Figure 2B. Surprisingly, the distribution is not a smooth curve as might have been expected, but to either side of the central peak (y = 0, the center of the ID), the plot is essentially linear, falling away to a finite value at each edge (y = 1, equivalent to the half-width of the ID). This finite value occurs because the slope of the membrane at the top of the peak is very large, although the radius is small. The relative height of the distribution at the middle and the edges is ~2.2:1. Clearly, this is a great simplification of a very complicated structure, but it provides a basis on which to interpret the immunofluorescence and immunogold data.

RESULTS

Structural Analysis of the ID Folds in the Interfibrillar Region

Figure 1 shows a longitudinal section of the ID in mouse left

ventricle. In the transverse regions of the ID, the axial extent of the corrugations or pleats (what we will loosely term the width of the ID) is variable, extending from 0.3 μm to well over 1 μm. The ordered sarcomeric arrangement of the myofibrils, seen most clearly in the A-bands, continues up to the ID. It is clear that the distance from the top of the folds (the edge of the ID) to the end of the A-band is similar to the length of the I-band between the end of the A-band and the Z-disc at the other end of the sarcomere. This is also indicated by the observation that the ID folds start at about the same position as the Z-disc in the neighboring fibril where there is a step (Figure 1A, arrows). There is, however, no obvious Z-disc structure at the junction between fibril and ID (Figure 1B, open arrow). Rather, the thin filaments continue into the adherens junctions (Figure 1, B and C). This is in agreement with evidence from stereo pairs of electron micrographs that show that the thin filaments are continuous through this region (Forbes and Sperelakis, 1985). Furthermore, Yamaguchi *et al*. (1988) examined heart muscle cells labeled with myosin S1 and showed that all the thin filaments in the terminal half-sarcomere and neighboring ID had the same polarity, i.e., with their barbed ends at the ID.

In addition to well-defined junctions, there are stretches of ID membrane with no known function that carry no obvious extra mass, called the general sarcolemma (Forbes and Sperelakis, 1985). These areas can occur anywhere on the ID membrane, but we observe that they often feature at the tips of the folds in the membrane (Figure 1B, arrowhead). We have investigated the organization of the general sarcolemma within the interfibrillar region in more detail using short sequential series of sections. If we consider the ID membrane to be a series of peaks and troughs, then the
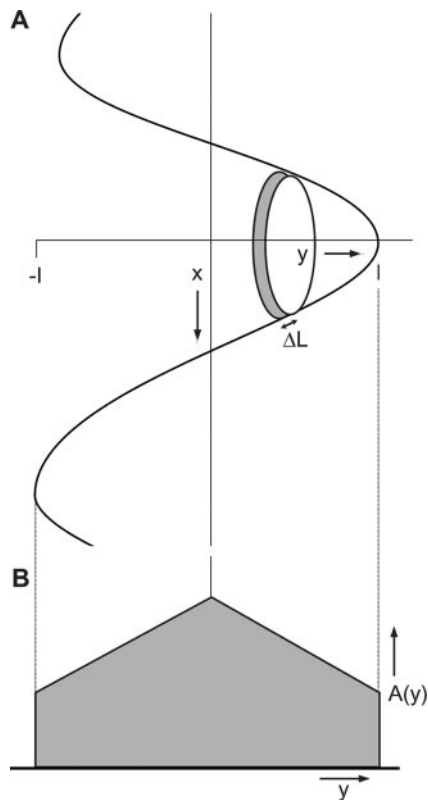
Figure 2. Diagram to illustrate the calculation of the area of the folded ID membrane at each axial level. (A) The membrane is approximated as a series of rounded cones with a sinusoidal section so that $y = \cos x$. At each axial level, y, a thin slice has an area $2\pi x \Delta L$, where L is the distance along the curve. (B) Calculated variation of area with axial distance, y.

slopes usually comprise adherens junctions, whereas the apex of essentially all the peaks is clear of the cytoplasmic plaque material. This is shown for one peak in Figure 1D.

Distribution of Spectrin in the ID

In our previous study of the distribution of αII-spectrin in cardiac tissue, we found by immunofluorescence that it had a strong presence in the ID (Bennett *et al.*, 2004). This is in agreement with Messina and Lemanski (1989) and Isayama *et al.* (1993). In contrast, we do not find αI-spectrin at the ID or within the cell (Figure 2, A–C; also see Baines and Pinder, 2005), although it is strong in the plasma membrane, like the αII isoform. This is contrary to previous reports by Messina and Lemanski (1989) and Isayama *et al.* (1993) that antibodies to erythrocyte, that is, αI-spectrin, label the ID.

When the αII-spectrin distribution in the ID was observed in more detail, as for example, in thin cryosections, it was seen to be split axially, lying closely apposed either side of the main bulk of the ID (Figure 3D). We have measured the position of these doublet stripes with respect to those at the Z-disc (Figure 4; see *Materials and Methods*). The measurements show that within a fibril, the distance of a single spectrin stripe at the ID from its nearest neighboring Z-disc is the same as the average spacing of the antibody Z-disc stripes in the same fibril, within measurement error of one or two pixels. Figure 4B shows this graphically as a plot of the measured versus the calculated distance between the doublet of αII-spectrin stripes at the ID. The points lie on a straight line of unit slope passing through
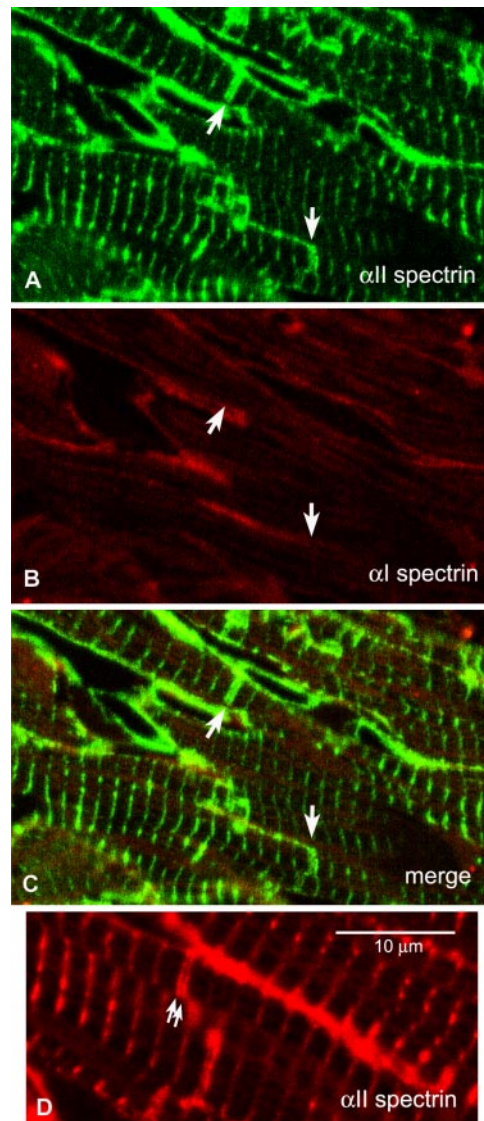
Figure 3. (A–C) Cryosections labeled with antibodies to spectrin αI and αII. Arrows indicate IDs that can be identified in αII labeled sections but not revealed by αI. (A) αII-spectrin. (B) αI-spectrin. (C) Combined image. (D) Thin section labeled with antibody to αII-spectrin showing the doublet labeling at the ID (arrows).

the origin (slope 1.08; intercept 0.08 μm), indicating that the relationship holds true regardless of ID width. Because spectrin is a membrane-associated cytoskeleton protein, this suggests that it partitions to a membrane compartment predominantly lying at the axial extreme of the ID.

The Relationship between the Distribution of Spectrin and Adherens Junction Proteins in the ID

To more accurately determine the distribution of spectrin in relation to the adherens junction proteins vinculin and β-catenin, we used electron microscopy of immunogold-labeled cryosections. Both proteins were predominantly found apposed to the ID membrane over most of its convoluted length (Figure 5, A and B). A similar distribution of vinculin has been shown before in chick cardiac muscle (Geiger *et al.*, 1980; Volk and Geiger, 1986). The gold particles mostly occur within the cytoplasmic edge of the dark plaque material that coats the
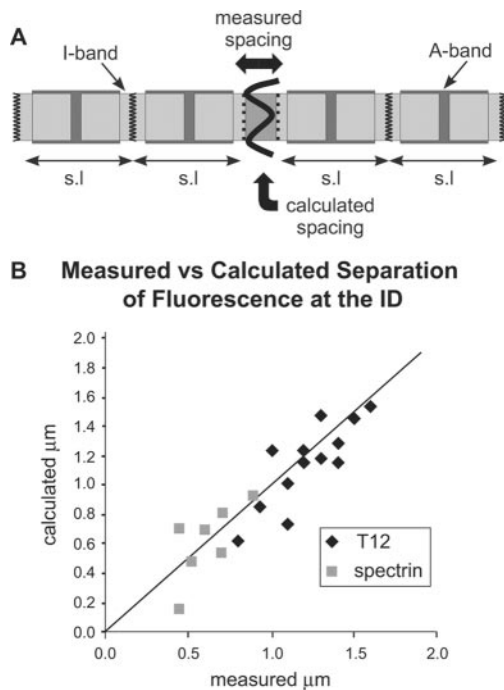
Figure 4. (A) Diagram of the folds of the intercalated disc and its associated myofibrils. Arrows show the how measured and calculated spacings of the fluorescent doublet across the ID were determined (see *Materials and Methods*). (B) Plot of the measured separation of the doublet against the calculated value for αII spectrin and titin T12 antibodies. The straight line passes through the origin and has a slope of 1.

membranes at the adherens junctions and not at the membrane itself. The β-catenin label, in contrast, is found much closer to the membrane. This is apparent from measurements of the

distance of the gold particles from the midline between the ID membranes of adjacent cells (Figure 6, A and B). The vinculin distribution is very similar to that shown by Volk and Geiger (1986); the average distance of particles is 50 nm, with 80% of the particles closer than 70 nm to the center of the midline. Assuming a separation of the membranes of ~20 nm, this suggests that vinculin occurs at a distance of ~40 nm from the cell membrane. For β-catenin, the distribution peaked near the membrane with 80% of the particles measured at <30 nm from the midline, thus positioning the protein at <20 nm from the membrane. These measurements are therefore consistent with the model for the adherens junction where transmembrane N-cadherin binds to vinculin via an α-catenin/β-catenin bridge, placing vinculin further from the membrane than β-catenin (for example, see Pokutta and Weis, 2002).

Spectrin shows a different distribution (Figure 5C). We have not found αII-spectrin in association with the gap junctions or the desmosomes. We have found it mostly associated with the strongly folded interfibrillary regions of the ID membrane, which are rich in adherens junctions. However, most of the label is found outside the cytoplasmic plaque of the adherens junctions and often associated with the tops of the folds on the ID. This is emphasized in Figure 5D in which a specimen is double labeled for spectrin and vinculin. Again, the vinculin is spread along the angled folds of the membrane. However, spectrin is more sparse, and the gold particles predominantly clump around the outer, convex folds in the membrane. There is little label on the inner, concave side of the bends. Measurements are less accurate because the definition and location of the membrane at the peaks is less clear for the general sarcolemma than the adherens junctions. As a result, the distance to the center of the membrane was found to vary between 0 and 200 nm with an average of 90 nm (Figure 6C).

To examine whether the distribution of the gold label was consistent with the immunofluorescence data, the axial distribution of the gold across the ID was measured. The center of the ID, as described in *Materials and Methods*, was deter-
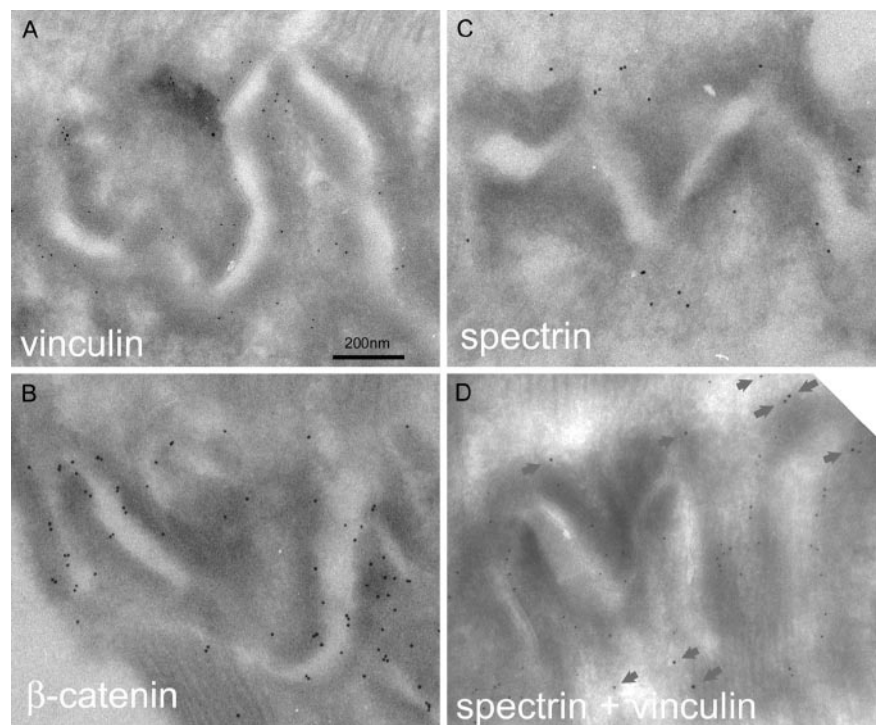
Figure 5. Electron micrographs of ID regions in cryosections immunogold labeled for vinculin (5-nm gold) (A), β-catenin (10-nm gold) (B), αII-spectrin (10-nm gold) (C), and vinculin (5-nm gold) and αII-spectrin (10-nm gold) (D). Arrows in D indicate the spectrin/gold label.
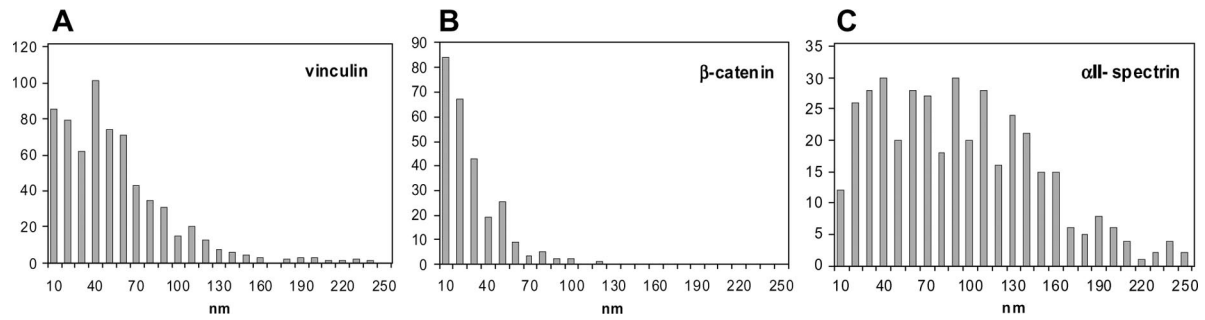
Figure 6. Histograms of the distance of the immunogold particles from the center of the ID plasma membrane doublet for vinculin (A), β-catenin (B), and αII-spectrin (C).

mined in relation to the two nearest neighboring Z-discs and M-bands, and the position of the gold particles was measured from that point. The width of the ID was taken to be the separation between the expected positions of the Z-discs, i.e., the ends of the terminal I-bands. Because ID widths vary, the data have been normalized to an ID width of 1000 to combine the data from several micrographs. The results are shown for vinculin, β-catenin, and spectrin in Figure 7. The vinculin and β-catenin data show single broad curves tailing off at about ±500. These distributions are very similar to the model calculation of the axial variation of the area of ID membrane shown in *Materials and Methods* and thus support the observation that the antigens seemed to be uniformly distributed over the surface of the membrane. In contrast, the αII-spectrin data give a bimodal peak, low at the center, with significant amplitude at ±500, the extreme edges of the ID. Thus, the immunogold data are consistent with the immunofluorescence and the modeling reinforces the conclusion that spectrin is not distributed along the folds of the ID but rather is concentrated at the axial edges of the ID at the tops of the folds.

Identification of the "Transitional Junction"

The above-mentioned observations raise the following question; how does the split αII-spectrin distribution relate to that of adjacent domains in the ID? In particular, because there is no obvious Z-disc at the ID fibril junction but the spectrin label indicates that this is the axial level at which it is found, how does αII-spectrin relate to Z-disc proteins? In this context, our previous work revealed that the fluores-

cence from a Z-disc-located titin antibody was also split at the ID (Bennett *et al.*, 2004). Therefore, we have investigated the apparent titin/spectrin colocalization at the ID in more detail as well as probing for other I-band sarcomeric proteins in the interfibrillar region.

Compared with the broad single stripe revealed by the immunolocalization of an antigen that follows the contours of the ID membrane, an antigen at the end of the A-band would show a doublet distribution across the ID. An example of such a difference in labeling is shown in Figure 8. In the section in Figure 8A labeled with an antibody to vinculin, immunofluorescence is strong on the plasma membrane at the lateral edges of the muscle cells and at the ID where it shows as a single broad band. In contrast, the titin antibody, I20/I22, binds to an epitope near the end of the A-band, which moves in association with the thick filament as the sarcomere contracts. Immunofluorescence shows I20/I22 labeling to be a doublet about the Z-line of variable spacing, depending on the sarcomere length (Linke *et al.*, 1998; Figure 8B). At the ID, lines of I20/I22 titin label are seen at either side of the vinculin stain (Figure 8C) with an increased separation consistent with the greater distance between the ends of the A-band in neighboring cells. The fluorescent lines that define titin are straight, in agreement with the good order of the A-band lying next to the ID, as shown by electron microscopy.

The other end of the elastic element of I-band titin is revealed by T12, an antibody that labels an epitope ~100 nm to either side of the Z-disc, a position that is unchanged over physiological sarcomere lengths. Figure 8, D–F, shows a
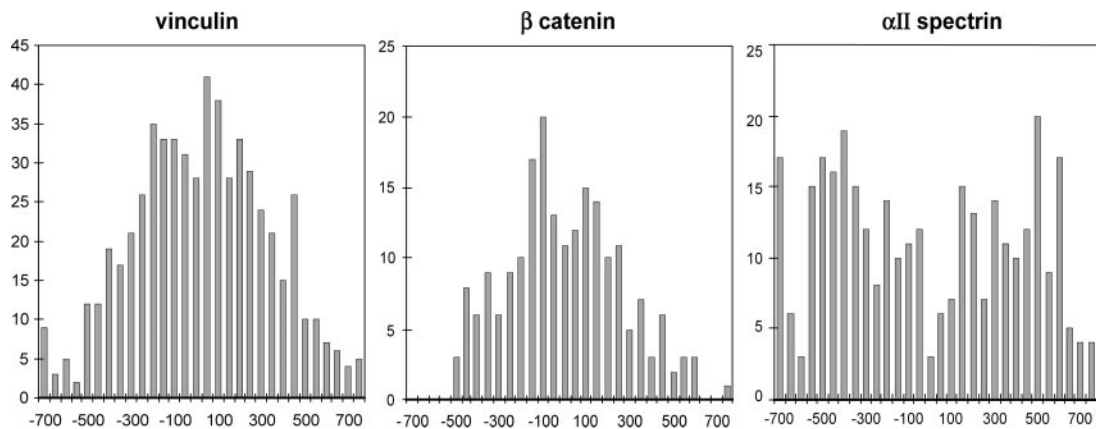
Figure 7. Axial distribution across the ID of the immunogold particles for vinculin (A), β-catenin (B), and αII-spectrin (C).
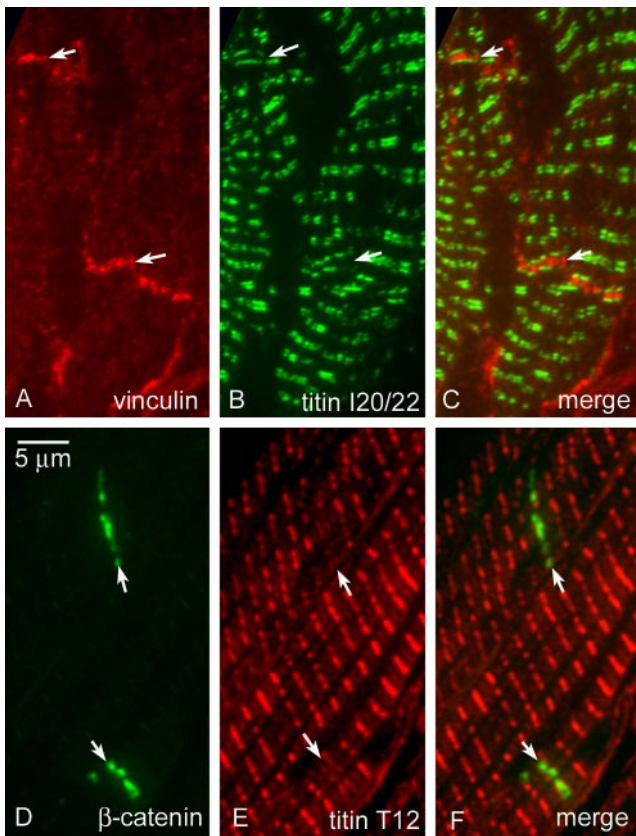
Figure 8. Immunofluorescence of double labeled cryosections. Section labeled for vinculin (A), titin I20/I22 (B), and combined image of A and B (C). Section labeled for β-catenin (D), titin T12 (E), and combined image of D and E (F). Arrows indicate intercalated discs.

section immunolabeled for both T12 and β-catenin. The broad fluorescent stripe of β-catenin is not split, consistent with its labeling close to the ID membrane (Figure 8D). T12 is visualized as a single line at the Z-disc (Figure 8, E and F). However, at the ID the T12 label is clearly split into two straight fine bands, suggesting that its position is not determined by that of the ID membrane (Figure 8F). It is also noticeable that the lines are weaker than the single stripes at the Z-disc. If, like β-catenin and vinculin, Z-disc titin were associated with the ends of the thin filaments at the ID membrane the T12 antibody would also label at the membrane and be imaged as a single broad stripe. This is not so. We have measured the spacing of the titin doublets at the ID and find that, like αII-spectrin, the values are the same as they would be if they lay at the predicted Z-disc position (Figure 4B). Again the values lie on a straight line of slope 1 (calculated slope 1.01, intercept −0.08 μm) and are independent of the ID width as determined by the doublet spacing. Therefore, titin lying closest to the ID maintains the same relationship with the end of the A-band as in the remainder of the fibril and its position is not governed by that of the ID.

In extension, other proteins associated with the Z-disc might be expected to have a doublet distribution across the ID. Antibody to sarcomeric α-actinin does indeed show a doublet (Figure 9, A–C). Like the titin T12 domain antibody, the position of the doublet lines is as would be expected with respect to the neighboring sarcomeres. Furthermore, the level of label is lower than at the Z-disc. The same results are found with an antibody against ZASP1 (homologous to mouse "cypher"), which binds to α-actinin at the Z-disc (our unpublished data; Faulkner *et al.*, 1999). Further evidence for a standard sarcomeric thin filament structure in the terminal sarcomere comes from labeling with an antibody to sarcomeric tropomyosin. This antibody labels the thin filaments in regions other than the Z-disc. Double labeling with β-catenin demonstrates that this isoform of tropomyosin is not present in the ID but does occur in the half-sarcomere
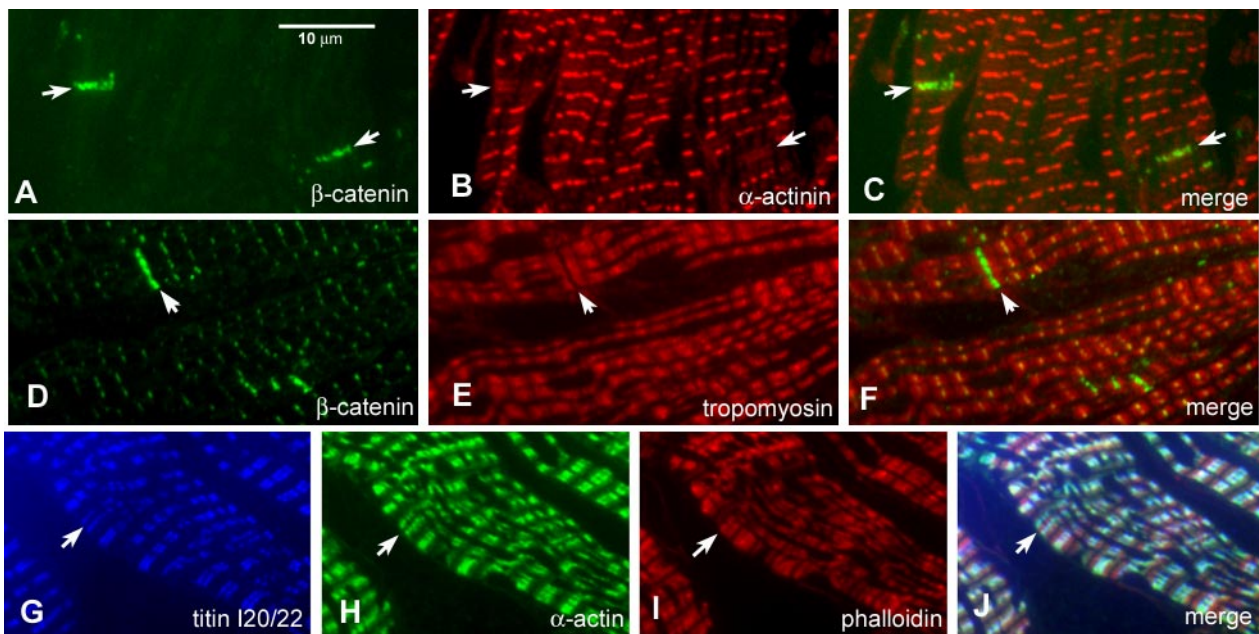
Figure 9. Immunofluorescence of double labeled cryosections. (A–C) Section labeled for β-catenin (A), for α-actinin (B), and combined image of A and B (C). (D–F) Section labeled for β-catenin (D), for tropomyosin (E), and the combined image of D and E (F). (G–J) Section labeled for titin T12 (G), cardiac α-actin (H), phalloidin (I), and merged image (J). Arrows indicate the intercalated discs.

immediately neighboring the ID (Figure 9, D–F). The same results were found with antibodies to cardiac troponin I (our unpublished data). We have also examined the distribution of actin around the ID. Figure 9, G–J, shows cardiac muscle labeled for cardiac α-actin and phalloidin and counterstained with antibodies to titin T12. The results show that cardiac α-actin is present within the sarcomeric I-bands but not at the ID. Phalloidin, however, also labels in the ID as well as the I-bands, indicating the presence of a different isoform of actin in the ID.

Our data therefore suggest that in the final half-sarcomere adjacent to the ID, there is a standard I-band that ends with a region that resembles a Z-disc in that N-terminal titin and α-actinin, recognized Z-disc markers, occur. We have named this region the "transitional junction." Beyond this region, toward the membrane of the ID, the actin and associated proteins of the thin filaments in the ID folds are not sarcomeric.

DISCUSSION

The "Transitional Junction"

The intercalated disc is critical for mechanical stability, transmission of electrical and chemical stimuli, and contractile force. For the latter, it is essential that there be effective structural and functional integration of the myofibrils with the adherens junctions. This is achieved by the thin filaments that emanate from the terminal half-sarcomere, continue into the ID sarcoplasm, and bind via vinculin to the adherens junction (Forbes and Sperelakis, 1985). Because several folds in the ID anchor any one fibril and the axial width of the ID varies considerably, thin filaments in this region accordingly vary considerably in length. This has repercussions regarding order in the thick filament array in the final sarcomere; even balance of the A-band is essential for generating uniform tension across and along the fibril. Regularity within sarcomeres is maintained by titin, the giant protein stretching from M-band to Z-disc that acts as a passive elastic element in the I-band (Horowits *et al.*, 1986; Wang *et al.*, 1991; Granzier and Irving, 1995; Labeit and Kolmerer, 1995). Should titin extend to the ends of the thin filaments at the ID membrane, it would exert different forces on each thick filament, and, contrary to observation, the resultant A-band would be highly disorganized. We find, however, that titin does not extend to the ID but rather, despite the absence of Z-disc–like structure, terminates at a point equivalent to the projected Z-disc. Conventional Z-disc components concentrate here, whereas I-band proteins in the terminal half-sarcomere are normally disposed. We name this domain the "transitional junction"; its protein arrangement is summarized in Figure 10. From our evidence, we surmise that actin filaments are cross-linked by α-actinin. The α-actinin cross-linkage was demonstrated to separate parallel actin filaments by more (38 nm) than antiparallel filaments (22 nm) (Liu *et al.*, 2004). This mirrors the greater separation observed between parallel filaments in the I-band compared with that seen for antiparallel Z-disc filaments. It follows that parallel thin filaments in the transitional junction may be cross-linked by α-actinin without alteration in spacing.

In our model titin overlaps α-actinin. Titin has multiple binding sites for α-actinin throughout its N-terminal (Gregorio *et al.*, 1998; Young *et al.*, 1998), whereas that part of titin proximal to the Z-disc associates with the thin filament (Linke *et al.*, 1997). These interactions are sufficient for the attachment of titin to the thin filament in the transitional junction. ZASP, a Z-disc-associated protein, is also expected to contribute to junc-
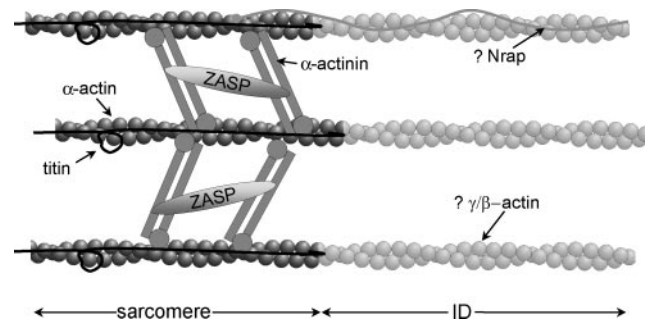
Figure 10. Diagram to show the possible arrangement of proteins in the transitional junction between fibril and ID. Sarcomeric α-actin is cross-linked by sarcomeric α-actinin, which also binds to ZASP. Beyond this point, the actin isoform changes, possibly to γ-actin. Within the sarcomeric domain titin is present and binds to the transitional junction through its interaction with actin and α-actinin. N-RAP, an actin binding protein is shown as a possible mediator of the transition.

tional stability through binding of its PDZ moiety to α-actinin (Faulkner *et al.*, 1999; Zhou *et al.*, 1999).

One self-evident feature of our immunofluorescence images supports our model. By comparison with the Z-disc, the fluorescence intensity of transitional junction proteins (titin, α-actinin, and ZASP) is reduced. This is expected because only half the number of actin filaments is present. Additionally, however, the relatively low electron density here indicates that many Z-disc–associated proteins are absent.

Beyond the transitional junction, the actin isoform in the thin filament changes seamlessly from α-cardiac actin. We are uncertain which isoform is present, nor how the transition is achieved, but we consider it significant that the actin- and α-actinin–binding protein N-RAP locates at the ID with a split distribution (Luo *et al.*, 1997; Zhang *et al.*, 2001). One possible arrangement for N-RAP is presented in Figure 10.

The Relationship of Adherens Junctions with the Spectrin-rich Domains

We conclude that, at the ID, there is physical separation of two critical functions of the Z-disc, that is, as an anchor for titin, discussed above, and as the transmitter of active tension via the adherens junctions at the plasma membrane. The dissociation of these functions results from the pronounced folding of the ID membrane in regions rich in adherens junctions. The myotendon junction of skeletal muscle has the same structure as the intercalated disc, with the myofibrils terminating at the level of the Z disc (but without a clearly defined Z-disc) and linking to an extended intermediate structure with pronounced folds where the muscle cells attach to collagen. Tidball (1983, 1991) argues that this allows the thin filaments to connect with the membrane at an acute angle so as to optimize the balance between shear and tensile loading, thereby enabling maximum adhesive force production. At the myotendinous junction, the angle between filament and membrane is low, ~4°. It follows that, in the heart, folding of the ID membrane allows for similar mechanics; the optimal position for thin filament attachment is along the slopes of the folds. This is indeed where adherens junctions concentrate.

Clearly, the bare zones at the tips of the ID membrane protrusions are not ideal for the purpose of tension transduction. Our evidence is that this region is rich in αII-spectrin. Previously, we suggested that αII-spectrin relates
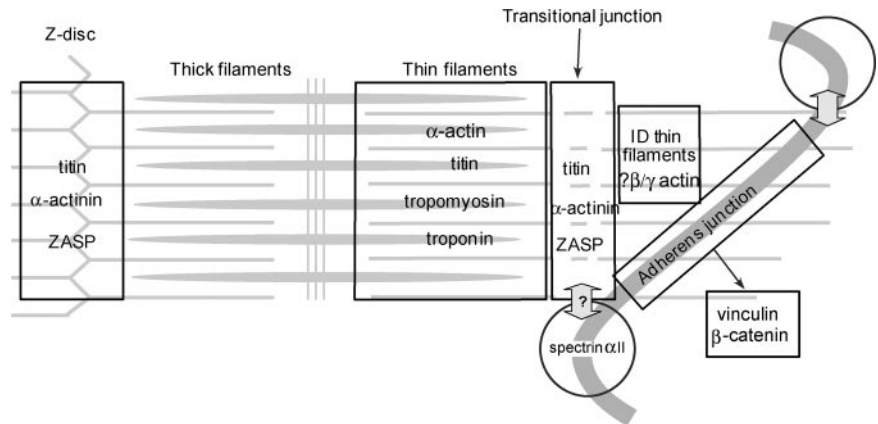
Figure 11. Diagram to show the distribution and relationship of the proteins investigated in the intercalated disc. Titin, α-actinin, and ZASP are found associated with the thin filament in the transitional junction between the final half-sarcomere and the ID thin filaments. The thin filaments ends are inserted into the adherens junctions. Spectrin found in a domain at the tops of the folds is well-positioned to interact with the proteins of the transitional junction.

to the sarcoplasmic reticulum at the edge of fibrils at the Z-disc (Bennett *et al.*, 2004). Because both sarcoplasmic reticulum and T-tubules also distribute at the ID, it is likely that spectrin fulfills an equivalent function there. Comparatively, the level of spectrin-associated fluorescence is greater at the ID than within the body of the cell, suggesting that spectrin fulfills an additional role at the ID. The fold curvature is reminiscent of the classical arrangement of spectrin in the erythrocyte where it, together with its associated proteins, maintains the structure and integrity of the cell membrane. By extension, therefore, we consider that spectrin is instrumental in creating and maintaining membrane peaks of the ID. The frequency of the apparent folds in the micrographs suggests that there will be a number of these peaks surrounding each fibril.

Our evidence is that βII-spectrin is present in the ID (Baines and Pinder, 2005), indicating the existence here of the most stable tetrameric form of spectrin, $(\alpha II\beta II)_2$ (Bignone and Baines, 2003). Isoforms of other cytoskeletal proteins involved in the erythrocyte spectrin network have also been identified at the ID, including two protein 4.1 isoforms, 4.1R and 4.1N (Baines and Pinder, 2005), and an ankyrin isoform, ANK G (Mohler *et al.*, 2004). In red blood cells, these proteins form a link between the actin cytoskeleton and (via ankyrin) a membrane channel, Band 3 (Bennett and Baines, 2001). Band 3 has also been identified as one of the membrane channels at the ID (Lima *et al.*, 2003). This supports a further role for the spectrin-based network in the ID as a link between the cytoskeleton and an ionic channel.

The Interaction between Spectrin and the Transitional Junction

We found that the bare tips of the ID membrane folds lie in proximity to the transitional junction and envisage scope for an interaction between the two, mediated by spectrin (shown diagrammatically in Figure 11). At the costamers of skeletal muscle, βI-spectrin colocalizes with MLP, thus linking spectrin through MLP to α-actinin (Flick and Konieczny, 2000). A similar interaction in heart would lock the spectrin-rich domain and transitional junction together and ensure that the ID extremities are constrained at the same axial position while additionally allowing communication between the ID membrane and myofibril. This might explain how loss of cardiac MLP leads to alterations in the ID structure (Ehler *et al.*, 2001).

An important consequence of our observations is that they provide insight into how a new sarcomere is added within the cell. It is thought that sarcomeres are added to growing

muscle fibers at their ends (Goldspink, 1972). The transitional junction allows for the insertion of a new sarcomere via separation of the actin filaments between the two actin isoforms, all without the reorganization of the ID. This process is of direct relevance to understanding DCM. This disease displays increased length of the cardiomyocytes brought about by the insertion of additional sarcomeres accompanied by structural changes at the ID with concomitant up-regulation of adherens junction proteins (Arber *et al.*, 1997; Sussman *et al.*, 1998; Ehler *et al.*, 2001).

REFERENCES

Arber, S., Hunter, J. J., Ross, J., Jr., Hongo, M., Sansig, G., Borg, J., Perriard, J. C., Chien, K. R., and Caroni, P. (1997). MLP-deficient mice exhibit a disruption of cardiac cytoarchitectural organization, dilated cardiomyopathy, and heart failure. Cell *88*, 393–403.

Baines, A. J., and Pinder, J. C. (2005). The spectrin-associated cytoskeleton in mammalian heart. Front. Biosci. *10*, 3020–3033.

Bennett, P. M., Baines, A. J., Lecomte, M. C., Maggs, A. M., and Pinder, J. C. (2004). Not just a plasma membrane protein: in cardiac muscle cells alpha-II spectrin also shows a close association with myofibrils. J. Muscle Res. Cell Motil. *25*, 119–126.

Bennett, V., and Baines, A. J. (2001). Spectrin and ankyrin-based pathways: metazoan inventions for integrating cells into tissues. Physiol. Rev. *81*, 1353–1392.

Bignone, P. A., and Baines, A. J. (2003). Spectrin alpha II and beta II isoforms interact with high affinity at the tetramerization site. Biochem. J. *374*, 613–624.

Ehler, E., Horowits, R., Zuppinger, C., Price, R. L., Perriard, E., Leu, M., Caroni, P., Sussman, M., Eppenberger, H. M., and Perriard, J. C. (2001). Alterations at the intercalated disc associated with the absence of muscle LIM protein. J. Cell Biol. *153*, 763–772.

Faulkner, G., *et al.* (1999). ZASP: a new Z-band alternatively spliced PDZ-motif protein. J. Cell Biol. *146*, 465–475.

Flick, M. J., and Konieczny, S. F. (2000). The muscle regulatory and structural protein MLP is a cytoskeletal binding partner of betaI-spectrin. J. Cell Sci. *113*, 1553–1564.

Forbes, M. S., and Sperelakis, N. (1985). Intercalated discs of mammalian heart: a review of structure and function. Tissue Cell *17*, 605–648.

Furst, D. O., Osborn, M., Nave, R., and Weber, K. (1988). The organization of titin filaments in the half-sarcomere revealed by monoclonal antibodies in immunoelectron microscopy: a map of ten nonrepetitive epitopes starting at the Z line extends close to the M line. J. Cell Biol. *106*, 1563–1572.

Geiger, B., Tokuyasu, K. T., Dutton, A. H., and Singer, S. J. (1980). Vinculin, an intracellular protein localized at specialized sites where microfilament bundles terminate at cell membranes. Proc. Natl. Acad. Sci. USA *77*, 4127–4131.

Goldspink, G. (1972). The Structure and Function of Muscle, ed. G. H. Bourne, New York: Academic Press, 181–236.

Granzier, H. L., and Irving, T. C. (1995). Passive tension in cardiac muscle: contribution of collagen, titin, microtubules, and intermediate filaments. Biophys. J. *68*, 1027–1044.

Gregorio, C. C., *et al.* (1998). The NH2 terminus of titin spans the Z-disc: its interaction with a novel 19-kD ligand (T-cap) is required for sarcomeric integrity. J. Cell Biol. *143*, 1013–1027.

Hayes, N. V., Scott, C., Heerkens, E., Ohanian, V., Maggs, A. M., Pinder, J. C., Kordeli, E., and Baines, A. J. (2000). Identification of a novel C-terminal variant of beta II spectrin: two isoforms of beta II spectrin have distinct intracellular locations and activities. J. Cell Sci. *113*, 2023–2034.

Horowits, R., Kempner, E. S., Bisher, M. E., and Podolsky, R. J. (1986). A physiological role for titin and nebulin in skeletal muscle. Nature *323*, 160–164.

Isayama, T., Goodman, S. R., and Zagon, I. S. (1993). Localization of spectrin isoforms in the adult mouse heart. Cell Tissue Res. *274*, 127–133.

Labeit, S., and Kolmerer, B. (1995). Titins: giant proteins in charge of muscle ultrastructure and elasticity. Science *270*, 293–296.

Lima, P.R.M., Salles, T.S.I., Costa, F. F., and Saad, S.T.O. (2003). α-Cardiac actin (*ACTC*) binds to the Band 3 (*AE1*) cardiac isoform. J. Cell. Biochem. *89*, 1215–1221.

Linke, W. A., Ivemeyer, M., Labeit, S., Hinssen, H., Ruegg, J. C., and Gautel, M. (1997). Actin-titin interaction in cardiac myofibrils: probing a physiological role. Biophys. J. *73*, 905–919.

Linke, W. A., Ivemeyer, M., Mundel, P., Stockmeier, M. R., and Kolmerer, B. (1998). Nature of PEVK-titin elasticity in skeletal muscle. Proc. Natl. Acad. Sci. USA *95*, 8052–8057.

Liu, J., Taylor, D. W., and Taylor, K. A. (2004). A 3-D reconstruction of smooth muscle alpha-actinin by CryoEm reveals two different conformations at the actin-binding region. J. Mol. Biol. *338*, 115–125.

Luo, G., Zhang, J. Q., Nguyen, T. P., Herrera, A. H., Paterson, B., and Horowits, R. (1997). Complete cDNA sequence and tissue localization of N-RAP, a novel nebulin-related protein of striated muscle. Cell Motil. Cytoskeleton *38*, 75–90.

Messina, D. A., and Lemanski, L. F. (1989). Immunocytochemical studies of spectrin in hamster cardiac tissue. Cell Motil. Cytoskeleton *12*, 139–149.

Mohler, P. J., Rivolta, I., Napolitano, C., LeMaillet, G., Lambert, S., Priori, S. G., and Bennett, V. (2004). Nav1.5 E1053K mutation causing Brugada syndrome blocks binding to ankyrin-G and expression of Nav1.5 on the surface of cardiomyocytes. Proc. Natl. Acad. Sci. USA *101*, 17533–17538.

Nicolas, G., Pedroni, S., Fournier, C., Gautero, H., Craescu, C., Dhermy, D., and Lecomte, M. C. (1998). Spectrin self-association site: characterization and study of beta-spectrin mutations associated with hereditary elliptocytosis. Biochem. J. *332*, 81–89.

Perriard, J.-C., Hirschy, A., and Ehler, E. (2003). Dilated cardiomyopathy: a disease of the intercalated disc? Trends Cardiovasc. Med. *13*, 30–38.

Pokutta, S., and Weis, W. I. (2002). The cytoplasmic face of cell contact sites. Curr. Opin. Struct. Biol. *12*, 255–262.

Radice, G. L., Rayburn, H., Matsunami, H., Knudsen, K. A., Takeichi, M., and Hynes, R. O. (1997). Developmental defects in mouse embryos lacking N-cadherin. Dev. Biol. *181*, 64–78.

Saggin, L., Gorza, L., Ausoni, S., and Schiaffino, S. (1989). Troponin I switching in the developing heart. J. Biol. Chem. *264*, 16299–16302.

Sussman, M. A., Welch, S., Cambon, N., Klevitsky, R., Hewett, T. E., Price, R., Witt, S. A., and Kimball, T. R. (1998). Myofibril degeneration caused by tropomodulin overexpression leads to dilated cardiomyopathy in juvenile mice. J. Clin. Investig. *101*, 51–61.

Tang, Y., Katuri, V., Dillner, A., Mishra, B., Deng, C. X., and Mishra, L. (2003). Disruption of transforming growth factor-beta signaling in ELF beta-spectrin-deficient mice. Science *299*, 574–577.

Tidball, J. G. (1983). The geometry of actin filament-membrane associations can modify adhesive strength of the myotendinous junction. Cell Motil. *3*, 439–447.

Tidball, J. G. (1991). Force transmission across muscle cell membranes. J. Biomech. *24* (suppl 1), 43–52.

Volk, T., and Geiger, B. (1986). A-CAM: a 135-kD receptor of intercellular adherens junctions. I. Immunoelectron microscopic localization and biochemical studies. J. Cell Biol. *103*, 1441–1450.

Wang, K., McCarter, R., Wright, J., Beverly, J., and Ramirez-Mitchell, R. (1991). Regulation of skeletal muscle stiffness and elasticity by titin isoforms: a test of the segmental extension model of resting tension. Proc. Natl. Acad. Sci. USA *88*, 7101–7105.

Yamaguchi, M., Yamano, S., Muguruma, M., and Robson, R. M. (1988). Polarity and length of actin filaments at the fascia adherens of the cardiac intercalated disc. J. Ultrastruct. Mol. Struct. Res. *100*, 235–244.

Young, P., Ferguson, C., Banuelos, S., and Gautel, M. (1998). Molecular structure of the sarcomeric Z-disc: two types of titin interactions lead to an asymmetrical sorting of alpha-actinin. EMBO J. *17*, 1614–1624.

Zhang, J. Q., Elzey, B., Williams, G., Lu, S., Law, D. J., and Horowits, R. (2001). Ultrastructural and biochemical localization of N-RAP at the interface between myofibrils and intercalated discs in the mouse heart. Biochemistry *40*, 14898–14906.

Zhou, Q., Ruiz-Lozano, P., Martone, M. E., and Chen, J. (1999). Cypher, a striated muscle-restricted PDZ and LIM domain-containing protein, binds to alpha-actinin-2 and protein kinase C. J. Biol. Chem. *274*, 19807–19813.